

SELF-CALIBRATION SYSTEM FOR THE ORIENTATION OF A VEHICLE CAMERA

Á. Catalá-Prat ^a, J. Rataj ^a, R. Reulke ^b

^aGerman Aerospace Center(DLR), Institute of Transportation Systems, Lilienthalplatz 7, 38108 Braunschweig, Germany
– (alvaro.catalaprat, juergen.rataj)@dlr.de

^bGerman Aerospace Center (DLR), Institute of Transport Research, Rutherfordstr.2, 12489 Berlin, Germany
– ralf.reulke@dlr.de

KEY WORDS: Camera, Calibration, Orientation, Orthorectification, Infrastructure

ABSTRACT:

The process of calibration is a prerequisite for each computer vision system. Calibration involves calculating both intrinsic and extrinsic parameters of the camera. While intrinsic parameters (focal length, principal point, etc.) are usually fixed, extrinsic ones (position and angles of the camera) have to be determined when the camera moves in relation to world coordinates. The calibration of the extrinsic parameters is usually performed with help of some reference objects or known measured points (GCP's) in the scene. In the case of a vehicle camera, where the coordinates refer to vehicle coordinates, not the extrinsic calibration but the alignment of the camera to the Inertial Measurement Unit (IMU) is necessary. This paper proposes a solution for determining the orientation of a vehicle camera in relation to the vehicle. This novel approach escapes from tedious laboratory setups and reference measurements. It benefits from a known property of the road's infrastructure, namely the parallelism of the road markers. For this reason lane markers are detected and transformed through a fast perspective removal (FPR) to an orthographic perspective. Newton's Method is used for searching an optimal parameter set for this transformation. The algorithm works under the assumptions that the calibration is performed when driving on a straight and flat segment and the lane markers are visible. It reaches very good performance (via parametrical instead of image transformations) and good accuracy for lateral detection of features in automotive applications (for depth information, the algorithm must be improved).

1. INTRODUCTION

1.1 Motivation

Computer vision has become one of the most important areas of investigation in many disciplines like robotics, medicine, industrial production and automotive. The extraction of useful information from camera images has proven to be a challenging but promising task. An accurate calibration of the cameras is a prerequisite for most computer vision systems, and especially for those which deal with 3D reconstruction.

Through the process of calibration, the relationship between a world point and an image point is defined in terms of some intrinsic and extrinsic parameters. The intrinsic parameters are the principal point, the focal length and the lens distortion. They are independent of the environment of the camera and usually do not change during the measurement (as long as the lenses do not refocus). On the other hand, the extrinsic parameters are position and angle of the camera related to world coordinates. Any movement of the camera with respect to the world reference system implies to determine the extrinsic parameters again (unless the movement is exactly known).

At the Institute of Transportation Systems (DLR) an experimental vehicle (the *ViewCar*, see Figure 1) has been created in order to investigate new advanced driver assistance systems (ADAS) (Vollrath, 2003). The *ViewCar* is equipped with a variety of sensors for recording the environment, such as a laser-scanner, a radar sensor, a positioning system (DGPS and IMU) and four cameras with a fixed orientation to the environment. In order to support the ADAS, the environment must be modelled based on the sensor data, and hence, all cameras need to be calibrated accurately.



Figure 1. The ViewCar

Since we are interested in the vehicle's environment, the center of the "world" coordinates will be placed on a characteristic point in the vehicle (e.g. middle frontal axis). For those applications where the relation to real world coordinates is also relevant (e.g. for road map based approaches), the positioning system of the car (DGPS+IMU) could be additionally used. In this case, the vehicle's coordinate system would be related to the body frame of the IMU. In this document, extrinsic calibration is reduced to the alignment between the photo coordinates and the view platform (IMU).

A common problem of vision systems (especially in automotive applications) is the loss of validity of the alignment parameters in the course of time due to vibrations and sudden movements. Ernst et al. (1999) shows the importance of an accurate calibration by means of two examples, a lane following and an obstacle detection systems.

Since extrinsic calibration is a tedious task and has to be done often, a self-calibration system represents an attractive solution. Moreover, a self-calibrating system has the advantage of being

able to be run online at any time (when fulfilling the prerequisites). By doing this, accurate results are ensured steadily.

The intrinsic parameters of the *ViewCar* cameras do not vary during the drive. Hence, we focus on the calibration of the extrinsic ones. Although both the camera position and orientation in the vehicle are important, this initial work only deals with orientation, which is more susceptible to changes. The self-calibration of the position is to be left for further work.

1.2 Structure of the Paper

The paper is arranged as follows. After the motivation for doing this work, a brief state of the art on extrinsic camera calibration is presented. Section 2 gives an overview of this solution; section 3 goes into detail of the main stages of the process; followed by section 4, presenting some experimental results of the algorithm. Finally, section 5 gives some conclusions and discusses some possibilities of future work.

1.3 State of the Art

A large number of different systems and methods for camera calibration have been developed. Camera calibration in photogrammetry was first developed in aerial photogrammetry. The calibration of terrestrial cameras was derived from these techniques. An overview can be found in Grün and Huang (2001).

Different models and methods are suggested and can be found in the literature, like Brown (1971) and Tsai (1986).

There are following different procedures for the determination of the interior orientation.

Experimental setup in a lab: The camera is mounted on a rotation tilt table. A light spot is imaged into infinity by a collimator. Each single pixel can be illuminated. This is a parameter free approach. For each pixel, the view angle can be determined in the object space (Schuster, 1994).

Known coordinates of reference objects: 3D location, dimensions and/or proportions are known, like points, chessboards or reference bars. The calibration usually requires accurate measurements and carefully controlled laboratory setups (Tsai, 1986). The result can be improved with different views of the reference objects and applying a bundle block adjustment approach (Fraser, 2000).

For a vehicle camera, the solutions proposed by Broggi et al. (2001) and by Ernst et al. (1999) use a painted field on a piece of road as reference and place the car exactly in front of it.

Self calibration: Camera self calibration uses point correspondences in multiple views, without needing interior and exterior orientation. The basic assumption is that the interior orientation remains invariant (Maybank & Faugeras, 1992).

Several approaches base on the movement of the camera, and use tracked features from images taken at different positions for the calibration. Luong and Faugeras (1997) use a camera with flexible orientation and assumes a static scene. Dron (1993) uses a camera translated along a fixed rail. All these methods

have to deal with the problem of correspondence between different images.

The objective of the work presented in this paper is to carry out the calibration of the camera orientation with regard to the vehicle's coordinate system in a fast way and without the need of a complex setup. For the method, laboratory setups, complex reference objects and multiple images were avoided. Instead, the road lane markers were used as reference. This method will be useful for any vehicle camera from which road markers are visible.

2. PROPOSED SOLUTION

The main idea of the proposed algorithm consists of performing a Newton's search through the camera parameters space until they prove to be correct. For testing the current parameters the lane markers are transformed to an orthographic projection (perspective removal). The removal of the perspective strongly depends on the camera parameters (and on a flat road). A good parameter set will provoke the inverted lane markers to be in parallel and aligned with the vehicle's main orientation.

For transforming the world to an orthographic projection, some authors use a mapping technique on the whole image like IPM (Inverse Perspective Mapping). This way, features can be analysed on the remapped image, as in Broggi et al. (2001). For our solution, we have decided to firstly extract the interesting features (road markers) and then do a fast perspective removal (FPR) on them. This sequence assures that the features are not being lost by remapping and also performs faster, as it avoids removing the perspective effect of the whole image plane.

Prior to the FPR, an appropriate camera image has to be acquired and prepared. Besides, the lane markers have to be detected and provided to the rest of the algorithm. The Hough transformation is performed for detecting all image lines. Then, lines corresponding to the lane markers are selected manually.

Since the vehicle is driving on a straight road, the Hough transformation is a good solution for line detection. Besides, Hough offers the attractive advantage of not being susceptible to partially occluded or shadowed lines, which often happens in driving situations.

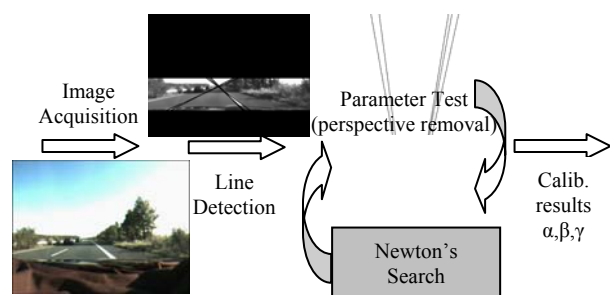


Figure 2. Overview of the process
Figure 2 shows an overview of the calibration process.

There are following assumptions for using this algorithm: the camera is mounted in the vehicle so that the road markers are visible; the vehicle is driving **on a flat** and **straight** road; and last, the vehicle drives **in parallel** to the road. Hence, the algorithm will only be executed on images that approximately fulfil these assumptions. Any deviation from the *perfect* flat and

straight road will result in noise of the calibration parameters. In section 4, some satisfactory experimental results are shown. However, it still remains necessary to run a detailed statistic analysis of the algorithm in order to study the impact of this noise on the accuracy of the calibration.

3. PROCESS DETAILS

3.1 Line Detection and Selection

The first task of the algorithm is to obtain the lines corresponding to the lane markers on the image. For doing this, the image is acquired and converted to grey scale. Besides, the upper and lower areas of the image are cut out, where there is only sky and the cockpit of the car. A Sobel edge filter is then passed through the image. As a result, all candidate points that possibly constitute straight lines (probably discontinuously) are obtained.

Next, the edge image is transformed into the Hough space. In this space each possible line is represented by (θ, d) , its angle and distance to origin, according to

$$x \cdot \cos \theta + y \cdot \sin \theta = d \quad (1)$$

Each point of the edge image increments the accumulator of all possible lines it could belong to in the Hough space, i.e., a sinusoidal curve. After having transformed all points, the actual lines of the original image are represented by the local maxima of the Hough space, which must be extracted from it.

Last in this stage, the road lines need to be distinguished from other noise lines. Currently, this selection is done manually by asking the user interactively about every line found. In most cases, the lane markers are not detected as a single line but as a bundle, which is not problematic to the algorithm (see section 4 for details). See Figure 3 for an example of an acquired image and the detected and selected lines.

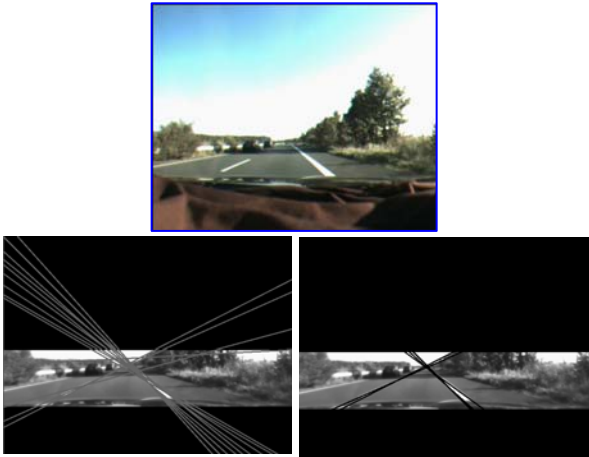


Figure 3. Acquired image, detected lines and selected lines

3.2 Fast Perspective Removal (FPR)

For testing the camera parameters, the perspective effect of the selected lines has to be removed and the slope of the resulting lines has to be checked. In the best case, these will be parallel to the driving direction.

The perspective removal, different to other work (Broggi et al., 2001), is not performed on the whole image, but only parametrically on the lines (FPR). For doing this, the pinhole camera model was used. In this model, a point of the world in homogeneous coordinates ($\mathbf{p}_w = [x_w \ y_w \ z_w \ 1]^t$) is acquired by the camera as a point in the image ($\mathbf{p}_i = [x_i \ y_i \ 1]^t$) according to next expression:

$$\mathbf{p}_i = \mathbf{M}_{\text{intrinsic}} \cdot \mathbf{M}_{\text{extrinsic}} \cdot \mathbf{p}_w \quad (2)$$

$$\begin{bmatrix} x_i \\ y_i \\ 1 \end{bmatrix} = \begin{bmatrix} c_x & f_x & 0 & 0 \\ c_y & 0 & f_y & 0 \\ 1 & 0 & 0 & 0 \end{bmatrix} \cdot \begin{bmatrix} \mathbf{R} & \mathbf{T} \\ 0 & 0 & 0 & 1 \end{bmatrix} \cdot \begin{bmatrix} x_w \\ y_w \\ z_w \\ 1 \end{bmatrix} \quad (3)$$

Here, the position of the principal point (c_x, c_y) and the focal length (f_x, f_y) are the intrinsic parameters of the camera (neglecting the radial and tangential distortions). The extrinsic parameters (actually the alignment parameters) are represented by both matrices, a rotation matrix \mathbf{R} depending on the orientation angles ω, ϕ and κ (respectively equivalent to roll, pitch and yaw) and a translation vector \mathbf{T} containing the projection center (longitudinally t_x , laterally t_y , and vertically t_z). Their expressions are:

$$\mathbf{R} = \begin{bmatrix} 1 & 0 & 0 \\ 0 & \cos \omega & \sin \omega \\ 0 & -\sin \omega & \cos \omega \end{bmatrix} \begin{bmatrix} \cos \phi & 0 & -\sin \phi \\ 0 & 1 & 0 \\ \sin \phi & 0 & \cos \phi \end{bmatrix} \begin{bmatrix} \cos \kappa & \sin \kappa & 0 \\ -\sin \kappa & \cos \kappa & 0 \\ 0 & 0 & 1 \end{bmatrix} \quad (4)$$

$$\mathbf{T} = [t_x \ t_y \ t_z]^t$$

For the aim of this work, both the intrinsic parameters and the position of the camera (\mathbf{T}) are assumed to be known and constant.

Since the combined matrix, $\mathbf{M} = \mathbf{M}_{\text{intrinsic}} \cdot \mathbf{M}_{\text{extrinsic}}$, is not square, it is not invertible. This is due to the ambiguity of the perspective transformation ($\mathbf{M}_{\text{intrinsic}}$). In order to be able to invert it, we must constrain the scene we are observing: since all lines considered lay in the road plane, the vertical position is a constant and can be included in the transformation matrix as follows:

$$\begin{bmatrix} x_i \\ y_i \\ 1 \end{bmatrix} = \begin{bmatrix} M_{11} & M_{12} & M_{13} & M_{14} \\ M_{21} & M_{22} & M_{23} & M_{24} \\ M_{31} & M_{32} & M_{33} & M_{34} \end{bmatrix} \cdot \begin{bmatrix} x_w \\ y_w \\ z_w = cte \\ 1 \end{bmatrix} \quad (5)$$

$$\begin{bmatrix} x_i \\ y_i \\ 1 \end{bmatrix} = \begin{bmatrix} M_{11} & M_{12} & (z_w \cdot M_{13} + M_{14}) \\ M_{21} & M_{22} & (z_w \cdot M_{23} + M_{24}) \\ M_{31} & M_{32} & (z_w \cdot M_{33} + M_{34}) \end{bmatrix} \cdot \begin{bmatrix} x_w \\ y_w \\ 1 \end{bmatrix}$$

The new transformation matrix \mathbf{M}' is invertible and can be used for removing the perspective effect from any image point by a single matrix multiplication:

$$\mathbf{p}_i = \mathbf{M}' \mathbf{p}_w \Rightarrow \mathbf{p}_w = \mathbf{M}'^{-1} \cdot \mathbf{p}_i \quad (6)$$

Given a line $\mathbf{l} = [A \ B \ C]^t$ (\mathbf{l}_i for an image line and \mathbf{l}_w for a road line),

$$\begin{bmatrix} A & B & C \end{bmatrix} \cdot \begin{bmatrix} x \\ y \\ 1 \end{bmatrix} = 0 \quad (7)$$

the perspective removal can be done according to the following expression:

$$\left. \begin{aligned} \mathbf{I}_i' \cdot \mathbf{p}_i = 0 \\ \mathbf{p}_i = \mathbf{M}' \mathbf{p}_w \end{aligned} \right\} \rightarrow \mathbf{I}_i' \cdot \mathbf{M}' \mathbf{p}_w = 0 \Rightarrow \mathbf{I}_w' = \mathbf{I}_i' \cdot \mathbf{M}' \quad (8)$$

Hence, no matrix inversion needs to be done. Next, Figure 4 shows an example of some image lines and the same lines after the perspective effect has been removed. As can be seen, the road lines in this example are not parallel, as the parameters have not been calibrated yet.

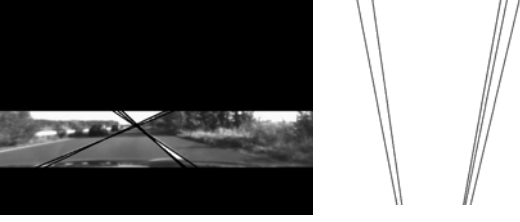


Figure 4. The detected lines before and after removing the perspective effect.

3.3 Search for the Correct Orientation Parameters

Once the lines can be quickly transformed into the road plane, the calibration of the camera orientation is reduced to a *minimum search* problem. If we can define a goodness function of a given parameter set, whose first and second derivative can be calculated, we will also be able to apply the Newton's method. This iterative method has the following expression for a multidimensional function:

$$\mathbf{p}_{k+1} = \mathbf{p}_k - \mathbf{v}f(\mathbf{p}_k) \cdot (\mathbf{H}f(\mathbf{p}_k))^{-1} \quad (9)$$

Where \mathbf{p}_k is the parameter set to find (in our case $[\omega \ \phi \ \kappa]$), $f(\mathbf{p}_k)$ is the goodness function to be minimized (defined later in this section), $\mathbf{v}f(\mathbf{p}_k)$ is the gradient vector of $f(\mathbf{p}_k)$ defined as

$$\mathbf{v}f(x_1 \dots x_n) = \left(\frac{\partial f}{\partial x_1}(x_1 \dots x_n) \quad \dots \quad \frac{\partial f}{\partial x_n}(x_1 \dots x_n) \right) \quad (10)$$

and $\mathbf{H}f(\mathbf{p}_k)$ is the Hessian matrix of the function f defined as:

$$\mathbf{H}f(x_1 \dots x_n) = \begin{pmatrix} \frac{\partial^2 f}{\partial x_1 \partial x_1}(x_1 \dots x_n) & \dots & \frac{\partial^2 f}{\partial x_1 \partial x_n}(x_1 \dots x_n) \\ \vdots & \ddots & \vdots \\ \frac{\partial^2 f}{\partial x_n \partial x_1}(x_1 \dots x_n) & \dots & \frac{\partial^2 f}{\partial x_n \partial x_n}(x_1 \dots x_n) \end{pmatrix} \quad (11)$$

For applying the method, the goodness function was defined as the sum of the slopes of the n road lines seen in an orthographic projection, which ideally should be 0. The smaller the function's value, the closer the parameter set is to the right calibration.

$$f(\omega, \phi, \kappa) = \sum_{i=1}^n \left(\frac{A_{wi}(\omega, \phi, \kappa)}{B_{wi}(\omega, \phi, \kappa)} \right)^2 \quad (12)$$

A_{wi} and B_{wi} are the components of the i^{th} line parametrically transformed to the road plane (through expression (8) seen in subsection 3.2). One can see that the first and second derivatives of $f(\omega, \phi, \kappa)$, though bulky, are easily calculable. As shown in section 4, this function provides good calibration results. See, as an example, the first partial derivative of $f(\omega, \phi, \kappa)$ with respect to ω . The rest of the first derivatives and the second ones are analogue.

$$\frac{\partial f(\omega, \phi, \kappa)}{\partial \omega} = \sum_{i=1}^n 2 \cdot \left(\frac{A_{wi}(\omega, \phi, \kappa)}{B_{wi}(\omega, \phi, \kappa)} \right) \cdot \left(\frac{\frac{\partial A_{wi}(\omega, \phi, \kappa)}{\partial \omega} \cdot B_{wi}(\omega, \phi, \kappa) - A_{wi}(\omega, \phi, \kappa) \cdot \frac{\partial B_{wi}(\omega, \phi, \kappa)}{\partial \omega}}{(B_{wi}(\omega, \phi, \kappa))^2} \right)$$

(13)

$$A_w(\omega, \phi, \kappa) = K_1 \cdot r_{11} + K_2 \cdot r_{21} + K_3 \cdot r_{31} \quad (14)$$

$$K_1 = A_i \cdot c_x + B_i \cdot c_y + C_i$$

$$K_2 = A_i \cdot f_x$$

$$K_3 = B_i \cdot f_y$$

$$r_{11} = \cos \phi \cos \kappa$$

$$r_{21} = \sin \omega \sin \phi \cos \kappa - \cos \omega \sin \kappa$$

$$r_{31} = \cos \omega \sin \phi \cos \kappa + \sin \omega \sin \kappa$$

$$\frac{\partial A_w(\omega, \phi, \kappa)}{\partial \omega} = K_2 \cdot (\cos \omega \sin \phi \cos \kappa + \sin \omega \sin \kappa) + K_3 \cdot (-\sin \omega \sin \phi \cos \kappa + \cos \omega \sin \kappa) \quad (16)$$

$$B_w(\omega, \phi, \kappa) = K_1 \cdot r_{12} + K_2 \cdot r_{22} + K_3 \cdot r_{32} \quad (17)$$

$$r_{12} = \cos \phi \sin \kappa$$

$$r_{22} = \sin \omega \sin \phi \sin \kappa + \cos \omega \cos \kappa$$

$$r_{32} = \cos \omega \sin \phi \sin \kappa - \sin \omega \cos \kappa$$

$$\frac{\partial B_w(\omega, \phi, \kappa)}{\partial \omega} = K_2 \cdot (\cos \omega \sin \phi \sin \kappa - \sin \omega \cos \kappa) + K_3 \cdot (-\sin \omega \sin \phi \sin \kappa - \cos \omega \sin \kappa) \quad (19)$$

The Newton's method also needs an initial approximation $\mathbf{p}_0 = (\omega_0, \phi_0, \kappa_0)$ of the parameters to be searched. If no significant changes were done, one can normally use the parameters found by the last calibration. Else, and for the first time, one can coarsely measure the orientation of the camera.

Last, for using the Newton's method one has to define an end-condition of the iteration. There are two different situations to consider: a good function's value was reached (compared with a reference value) or the function's value is stable.

4. EXPERIMENTAL RESULTS

4.1 Experiments Execution

The first experiments have been carried out on the frontal central camera of the *ViewCar*, a CCD camera with a resolution of 640x480 pixels. The coordinate system of the camera was defined as being in parallel to the vehicle's one. Thus, the driving direction corresponds to x (orientation around x is ω , equivalent to *roll*), the lateral direction corresponds to y (orientation around y is ϕ , equivalent to *pitch*) and the vertical direction corresponds to z (orientation around z is κ , equivalent to *yaw*). For the tests, some video sequences recorded during normal drives were used. The algorithm was run on numerous images of the sequences. For checking the correctness of the

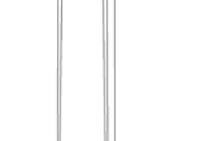
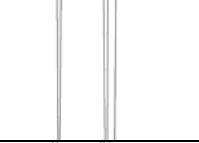
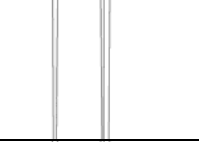
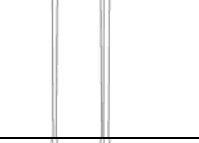
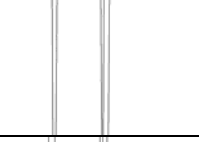
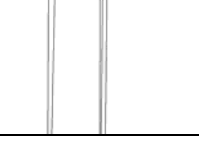
	
Original Image	
	Step 0: $\omega = 0^\circ$ $\phi = 0^\circ$ $\kappa = 0^\circ$ $f(\omega, \phi, \kappa) = 0,186489$
	Step 1: $\omega = -0,22^\circ$ $\phi = -6,12^\circ$ $\kappa = 3,31^\circ$ $f(\omega, \phi, \kappa) = 0,000735$
	Step 2: $\omega = 10,29^\circ$ $\phi = -6,87^\circ$ $\kappa = 2,60^\circ$ $f(\omega, \phi, \kappa) = 0,000591$
	Step 3: $\omega = 10,75^\circ$ $\phi = -6,64^\circ$ $\kappa = 2,55^\circ$ $f(\omega, \phi, \kappa) = 0,000311$
	Step 4: $\omega = 4,72^\circ$ $\phi = -6,36^\circ$ $\kappa = 3,26^\circ$ $f(\omega, \phi, \kappa) = 0,000287$
	Step 5: $\omega = 4,42^\circ$ $\phi = -6,31^\circ$ $\kappa = 3,28^\circ$ $f(\omega, \phi, \kappa) = 0,00028$
	Step 6: $\omega = 4,17^\circ$ $\phi = -6,29^\circ$ $\kappa = 3,30^\circ$ $f(\omega, \phi, \kappa) = 0,000281$
Stable value reached!	

Figure 5. First example of execution

results, the calibration parameters were applied to the existing lane detection system.

The results of two executions on different images of the same drive are shown in Figure 5 and Figure 6. In both, the initial approximation is set to 0° for all three orientation angles, ω , ϕ and κ . The examples are presented as a sequence of steps of the algorithm. For each step both the values of the parameters and the value of the goodness function are shown. The first example is also accompanied by a graphic of the lines without the perspective effect.

	
Original Image	
Step 0:	$\omega = 0^\circ$ $\phi = 0^\circ$ $\kappa = 0^\circ$ $f(\omega, \phi, \kappa) = 0,0725958$
Step 1:	$\omega = -8,91^\circ$ $\phi = -7,59^\circ$ $\kappa = 1,37^\circ$ $f(\omega, \phi, \kappa) = 0,035388$
Step 2:	$\omega = 1,15^\circ$ $\phi = -10,16^\circ$ $\kappa = 5,89^\circ$ $f(\omega, \phi, \kappa) = 0,0264104$
Step 3:	$\omega = -1,79^\circ$ $\phi = -5,83^\circ$ $\kappa = 4,81^\circ$ $f(\omega, \phi, \kappa) = 0,0008272$
Step 4:	$\omega = 5,34^\circ$ $\phi = -6,34^\circ$ $\kappa = 3,19^\circ$ $f(\omega, \phi, \kappa) = 0,0000885$
Step 5:	$\omega = 6,93^\circ$ $\phi = -6,65^\circ$ $\kappa = 3,01^\circ$ $f(\omega, \phi, \kappa) = 0,0000004$
Step 6:	$\omega = 5,88^\circ$ $\phi = -6,60^\circ$ $\kappa = 3,11^\circ$ $f(\omega, \phi, \kappa) = 0,00000005$
Stable value reached!	

Figure 6. Second example of execution

4.2 Experiments Evaluation: Performance, Accuracy and Availability

The first example, graphically, seems to reach very rapidly a good value. However, the algorithm manages to improve the results until a minimum of the goodness function is achieved. In the following, some remarks on performance, accuracy and availability of the algorithm are given.

The experimental results show that the calibration process needs about 6 steps of the Newton's iteration, which is a good **performance**. It is remarkable that each step only consists of parametrically transforming the n lines (n matrix multiplications) and calculating the gradient and Hessian matrices of $f(\omega, \phi, \kappa)$ for advancing the search. No image operators are carried out during the search.

Regarding the **accuracy**, these two examples show a difference lower than 2° for ω (equiv. roll), $0,3^\circ$ for ϕ (equiv. pitch) and $0,2^\circ$ for κ (equiv. yaw). The pitch and yaw angles show that the driving direction of the vehicle with respect to the lane is kept almost in parallel. For the roll angle, the experimental results do not converge as expected. There are some reasons for this. First, the orientation of the test camera was very close to pitch 0° and yaw 0° . In case they were exactly 0° , the value of the goodness function would be completely independent of the roll angle, and no minimum could be found. Thus, the more separated the orientation from 0° , the better the calibration can be done by our approach. Second, the orientation of the vehicle (recorded

by the IMU) is slightly different in both instants. Third, the line detector provides slightly shifted lines in relation to the actual lane markers, which also affects the calibration directly.

Some calculations (but no complete statistics yet) have been done in order to evaluate the accuracy reached by this first proposal. First, a point of the road plane located in a typical distance of 50m from the camera was projected into the image plane according to the parameter sets from both examples (Figure 5 and Figure 6). A difference of half pixel laterally and one pixel vertically was detected. Then, the inverted transformation was also tested. An image point was transformed into the road plane according to the parameter sets from both examples. The results show a lateral difference of about 1mm but also a big difference in the depth of about 10m. This effect is a result of the imaging geometry of the camera.

The **availability** of the system also plays a decisive role. By the test runs one has realized that the lighting and visibility conditions are crucial for obtaining good results. If the lane markers detected do not exactly coincide with the real ones, the procedure can turn to look for a maximum instead of a minimum of the goodness function. This is, actually, the most important aspect to improve concerning the algorithm in the future.

5. CONCLUSIONS AND OUTLOOK

In this paper a solution has been presented for calculating the orientation parameters of a vehicle camera. In the bibliography, no other methods using the structure of a standard road as reference for the calibration (or alignment determination) were found. In this first approach to the self-calibration, the parallelism of the lane markers was used as calibrating information. For applying this principle, a line detector, a fast perspective removal (FPR) and a Newton's search were implemented.

The principle has proven to be correct and to offer promising calibration results with very good time performance. In this sense, it is remarkable that image operators were avoided and parametrical transformations were preferred.

Nevertheless, from the few tests that have already been carried out, some weak points were also recognized. Below, some of them are listed and some future solutions are proposed. A prerequisite before starting with the improvements will be a detailed statistical analysis of the algorithm's behaviour.

A first problem detected is that the algorithm does not work properly if the pitch and yaw orientations are too close to 0°. For solving this, the reference coordinate system should be changed to an optimal one in the future.

Besides, the algorithm strongly depends on a reliable line extraction, which is not yet available. In order to improve the line detector, this algorithm could be combined with the existing lane detector, so that a mutual support of either system could be achieved.

The algorithm could also be made more robust in the future by adding other image features to the goodness criterion, such as distance information between lines, vertical features like light or electrical poles, building edges, or other horizontal lines, e.g. from other vehicles.

Last, it is also important to check how much influence the vehicle's own movement and orientation have (i.e., noise). For analysing this, the measurements from the IMU will be used in the future.

In conclusion, this implementation of a self-calibration principle for a vehicle camera has proven to be very promising. Future work, applications and tests (with help of the positioning system) will be continued on the *ViewCar*, at the Institute of Transportation Systems, at the German Aerospace Center (DLR).

REFERENCES

- Broggi, A., Bertozzi, M., Fascioli, A., 2001. Self-Calibration of a Stereo Vision System for Automotive Applications. In: *Procs. IEEE Int. Conf. on Robotics and Automation*, Seoul, Korea, Vol. 4, pp. 3698-3703.
- Brown, D.C., 1971. Close-range camera calibration. *Photogrammetric Engineering*, 37(8), pp. 855-866.
- Dron, L., 1993. Dynamic Camera Self-Calibration from Controlled Motion Sequences. In: *Procs. IEEE Comp. Soc. Conf. on Computer Vision and Pattern Recognition*, New York, USA, pp. 501-506.
- Ernst, S., Stiller, C., Goldbeck, J., Roessig, C., 1999. Camera Calibration for Lane and Obstacle Detection. In: *Procs. IEEE Int. Conf. on Intelligent Transportation Systems*, Tokyo, Japan, pp. 356-361.
- Fraser, E., 2000. Design and Implementation of a Computational Processing System for Off-Line Digital Close-Range Photogrammetry. *ISPRS Journal of Photogrammetry & Remote Sensing*, 55(2), pp. 94-104.
- Grün, A., Huang, T., 2001. *Calibration and orientation of cameras in computer vision*. Springer series in information science.
- Luong, Q.T., Faugeras, O.D., 1997. Self-Calibration of a Moving Camera from Point Correspondences and Fundamental Matrices. *International Journal of Computer Vision*, Vol. 22, pp. 261-289.
- Maybank, S., Faugeras, O.D., 1992. A theory of selfcalibration of a moving camera. *IJCV*, 8(2), pp. 123-151.
- Schuster, R., 1994. Sensor calibration and geometric calibration of a three line stereo camera. In: *International Archives of Photogrammetry and Remote Sensing*, Como, Italy, Vol. 30, pp. 265-271.
- Tsai, R.Y., 1986. An efficient and accurate camera calibration technique for 3D machine vision. In: *Procs CVPR'86 (IEEE Computer Society Conference on Computer Vision and Pattern Recognition)*, Miami Beach, FL.
- Vollrath, M., 2003. ViewCar- Freude am Fahren mit innovativen Assistenzsystemen. *DLR Nachrichten*, 106 – Sonderheft Verkehr, pp. 64-71.